NEOPLASIA
www.neoplasia.com

Volume 14 Number 2 February 2012 pp. 141–149 141

CLCA2 as a p53-Inducible Senescence Mediator[1,2]

Chizu Tanikawa*, Hidewaki Nakagawa†, Yoichi Furukawa‡, Yusuke Nakamura* and Koichi Matsuda*

*Laboratory of Molecular Medicine, Human Genome Center, Institute of Medical Science, The University of Tokyo, Tokyo, Japan; †Laboratory for Biomarker Development, Center for Genomic Medicine, RIKEN, Tokyo, Japan; ‡Division of Clinical Genome Research, Institute of Medical Science, The University of Tokyo, Tokyo, Japan

Abstract

p53 is a tumor suppressor gene that is frequently mutated in multiple cancer tissues. Activated p53 protein regulates its downstream genes and subsequently inhibits malignant transformation by inducing cell cycle arrest, apoptosis, DNA repair, and senescence. However, genes involved in the p53-mediated senescence pathway are not yet fully elucidated. Through the screening of two genome-wide expression profile data sets, one for cells in which exogenous p53 was introduced and the other for senescent fibroblasts, we have identified chloride channel accessory 2 (CLCA2) as a p53-inducible senescence-associated gene. *CLCA2* was remarkably induced by replicative senescence as well as oxidative stress in a p53-dependent manner. We also found that ectopically expressed CLCA2 induced cellular senescence, and the down-regulation of CLCA2 by small interfering RNA caused inhibition of oxidative stress–induced senescence. Interestingly, the reduced expression of *CLCA2* was frequently observed in various kinds of cancers including prostate cancer, whereas its expression was not affected in precancerous prostatic intraepithelial neoplasia. Thus, our findings suggest a crucial role of p53/CLCA2–mediated senescence induction as a barrier for malignant transformation.

Neoplasia (2012) 14, 141–149

Introduction

In nearly half of all human cancers, the *p53* gene is mutated or deleted [1]. The p53 protein is induced and activated in the nucleus by a variety of genotoxic stress such as DNA damage, hypoxia, and oxidative stress [2]. Activated p53 functions as a transcriptional factor, inhibits cell growth, and suppresses tumor formation by regulating many genes involved in cell cycle, apoptosis, and cellular senescence [3,4]. Although nearly a hundred p53-inducible genes have been identified so far [5,6], our recent microarray analysis revealed that there are still more than 50 p53-inducible genes that have not been well characterized yet [7]. To provide the detailed critical biologic functions of p53, we have previously identified a number of p53 target genes, such as *p53R2*, *p53AIP1*, *p53RDL1*, and *PADI4* [4,8–13].

Senescence is mainly regulated through two major pathways involving $p16^{Ink4a}$/Rb and $p14^{ARF}$/p53 [14,15]. Expression of $p16^{Ink4a}$ markedly increases with aging in mouse and human tissues [16,17]. In addition, $p16^{Ink4a}$ expression was shown to increase in senescent fibroblasts [18] as well as in response to oxidative stress or DNA damage [19,20]. $p16^{INK4A}$ functions as a CDK4/CDK6 inhibitor and subsequently leads to a G_1 arrest through the regulation of the pRB-E2F pathway [21,22].

Conversely, $p14^{ARF}$ controls the level of p53 by inhibiting the p53-specific ubiquitin ligase MDM2 [21,22]. The role of p53 in cellular senescence was clearly demonstrated by the fact that p53-deficient fibroblasts showed resistance to senescence [23]. In addition,

Address all correspondence to: Associate Professor Koichi Matsuda, Laboratory of Molecular Medicine, Institute of Medical Science, The University of Tokyo, 4-6-1, Shirokanedai, Minato, Tokyo 1088639, Japan. E-mail: koichima@ims.u-tokyo.ac.jp

[1]This work was supported in part by grant 18687012 from the Japan Society for the Promotion of Science and Ministry of Education, Culture, Sports, Science, and Technology of Japan (to K.M.). The authors declare no conflict of interest.

[2]This article refers to supplementary materials, which are designated by Tables W1 to W3 and Figures W1 to W4 and are available online at www.neoplasia.com.

Received 5 December 2011; Revised 6 February 2012; Accepted 10 February 2012

Copyright © 2012 Neoplasia Press, Inc. All rights reserved 1522-8002/12/$25.00
DOI 10.1593/neo.111700

reactivation of p53 in murine liver carcinoma cells induced tumor regression through the induction of cellular senescence [24], and mice expressing active mutant p53 displayed an early onset of aging phenotypes [25]. Hence, it is obvious that activated p53 prevents malignant transformation of damaged cells by inducing senescence [26]. Because cellular senescence was observed in precancerous tissues [27,28], senescence is likely to function as a barrier for malignant transformation in the carcinogenesis process [29].

Among a number of transcriptional targets of p53, $p21^{WAF1}$ was shown to play a principle role in both p53-dependent and independent senescence pathways [30]. $p21^{WAF1}$ inhibits cell cycle progression through interaction with the cyclin-CDK complex. However, because $p21^{WAF1}$-null fibroblast presents senescent phenotype [31], it is considered that another p53 target gene(s) may play a pivotal role in p53-dependent senescence induction. In this study, to identify a novel p53 target gene(s) that is essential for p53-dependent senescence induction, we examined the data sets of two genome-wide expression profile analyses. One data set was obtained using cells in which wild-type p53 was exogenously introduced, and the other was obtained using normal human dermal fibroblast (NHDF) cells at several time points from low to high passage (senescent state). Through this screening and subsequent biologic analysis, here we demonstrate a possible role of CLCA2 as a p53-inducible senescence mediator. We also examined the expression of CLCA2 in various cancer tissues. CLCA2 was reported as a p53 target gene that regulates p53-induced apoptotic pathway [32]. In addition, CLCA2 was shown to be downregulated or mutated in breast cancer tissues [33,34]. Recently, Rovillain et al. [35] reported that CLCA2 was strongly induced during senescence. Our findings would further support the crucial role of CLCA2 in the regulation of the senescence pathway as well as human carcinogenesis.

Materials and Methods

Complementary DNA Microarray

Complementary DNA (cDNA) microarray analysis was carried out as previously described [36]. For the senescence microarray, the total RNA of each sample was isolated and amplified using RNeasy spin column kits (Qiagen, Valencia, CA) and T7-Transcription kit (Epicentre Technologies, Madison, MI). For the p53 microarray, poly(A)+ RNAs were isolated from U373MG cells using a standard protocol. Each RNA sample was labeled and hybridized to a microarray consisting of 36,864 cDNA fragments (http://www.ncbi.nlm.nih.gov/geo/index.cgi, Accession No. GSE14953).

Plasmid Construction

The entire coding sequence of *CLCA2* cDNA was amplified by polymerase chain reaction (PCR) using KOD-Plus DNA polymerase (Toyobo, Osaka, Japan) and inserted into pCAGGS vector, which carries a gene conferring neomycin resistance. A Flag epitope tag was placed at the C-terminus of the CLCA2 expression vector. Constructs were confirmed by sequencing.

Cell Culture and Transfections

Each cell line was purchased from American Type Culture Collection, Lonza Biologics, Inc, or Japanese Collection of Research Bioresources. p53-deficient mice were obtained from RIKEN (http://www.cdb.riken.go.jp/arg/, Accession No. CDB0001K) [37]. We prepared mouse embryonic fibroblasts (MEFs) from embryonic day 13.5 embryos by standard protocols and maintained them in Dulbecco modified Eagle medium containing 10% fetal bovine serum. Replication-deficient recombinant adenovirus encoding p53 (Ad-p53) or LacZ (Ad-LacZ) was generated and purified, as previously described [8]. U373MG or H1299 cells were infected with viral solutions at an indicated multiplicity of infection (MOI) and incubated at 37°C until the time of harvest. Cells were transfected with plasmids using FuGENE6 (Roche, Basel, Switzerland). Small interfering RNA (siRNA) oligonucleotides, commercially synthesized by Sigma Genosis (The Woodlands, TX), were transfected with LipofectAMINE 2000 reagent (Life Technologies, Grand Island, NY) for 4 hours. Sequences of oligonucleotides are shown in Table W3. For treatment with genotoxic stress, cells were continuously incubated with hydrogen peroxide (H_2O_2) or adriamycin for 2 hours or irradiated by γ-ray or ultraviolet as indicated in the respective figure legends. 5-Aza-2′-deoxycytidine (5-Aza) and trichostatin A (TSA) were purchased from Sigma.

Quantitative Real-time PCR and Northern Blot Analysis

Isolation of total RNA from cultured cells was performed using RNeasy spin column kits (Qiagen) according to the manufacturer's instructions. Prostate and colorectal cancer tissues were prepared as previously described [38], and the total RNA of each sample was isolated and amplified. cDNAs were synthesized with the SuperScript Preamplification System (Invitrogen). Quantitative real-time PCR was conducted using the SYBR Green I Master or Probe Master on a LightCycler 480 (Roche) according to the manufacturer's recommendations. *β2-Microglobulin* or *β-actin* was used for normalization of expression levels. For the Northern blot analysis, a 2-μg aliquot of each poly(A)+ RNA was separated on a 1% agarose gel and transferred to nylon membrane by standard procedures. Hybridization with a random-primed ^{32}P-labeled CLCA2 cDNA probe was carried out according to the manufacturer's instructions. The primer and probe sequences are indicated in Table W3.

Gene Reporter Assay

DNA fragments, including potential p53-binding sites of mouse Clca5, were amplified and subcloned into pGL3-promoter vector (Promega, Madison, WI). To make a series of mutant vectors, a point mutation "T" was inserted into the site of the 4th, the 7th, the 14th, and the 17th nucleotides of the consensus p53-BS using inverse PCR methods. Reporter assay was performed using the Dual Luciferase Assay System (Promega) as described previously [8].

Antibodies

Rabbits were immunized with the recombinant proteins corresponding to the extracellular domain (amino acids 253-899) of CLCA2. Anti-Flag monoclonal (clone M2) and polyclonal (F7425) antibodies, as well as anti–β-actin monoclonal antibody (clone AC15) were purchased from Sigma. Mouse monoclonal anti-p53 (clone DO-1) and anti-$p21^{WAF1}$ (clone EA10) antibodies were purchased from Calbiochem (San Diego, CA). Anti-HA monoclonal antibody (F-7) was purchased from Santa Cruz Biotechnology, Santa Cruz, CA.

Western Blot Analysis

To prepare whole-cell lysates, cells were collected and lysed in chilled RIPA buffer (50 mM Tris-HCl at pH 8.0, 150 mM sodium chloride, 0.1% SDS, 0.5% DOC, 1% NP-40, and 1 mM phenyl methylsulfonyl fluoride) for 30 minutes on ice and centrifuged at 16,000*g* for 15 minutes. To concentrate the media, they were mixed with an equal volume of acetone and kept at −80°C for 1 hour. The

mixture was then centrifuged at 16,000*g* for 15 minutes, and the resulting protein pellets were dissolved in SDS sample buffer. Samples were subjected to SDS-PAGE and immunoblot analysis by a standard procedure. Silver staining was carried out using SilverQuest Staining Kit (Invitrogen) according to the manufacturer's instructions.

Immunocytochemistry

Adherent cells were fixed with 4% paraformaldehyde in phosphate-buffered saline (PBS) and permeabilized with 0.2% Triton X-100 in PBS for 5 minutes at room temperature. The cells were then covered with blocking solution (3% bovine serum albumin/PBS containing 0.2% Triton X-100) for 30 minutes at room temperature and incubated with rabbit anti-Flag antibody and mouse anti-HA antibody in blocking solution for 60 minutes at room temperature. Primary antibodies were stained with Alexa Fluor 488 antirabbit immunoglobulin G and Alexa Fluor 594 antimouse immunoglobulin G for 1 hour at room temperature and stained with 4′,6-diamidino-2-phenylindole, dihydrochloride (DAPI). For cell surface staining, cells were labeled under nonpermeabilized conditions using the buffer without Triton X-100.

Cell Proliferation and Cell Death Assay

Colony formation assays were carried out in six-well culture plates. Cells transfected with pCAGGS/CLCA2 or control plasmid were cultured in the presence of geneticin (Invitrogen) for 2 weeks. As a control plasmid, the entire coding sequence of CLCA2 cDNA was inserted into the vector in the opposite direction. Colonies were stained with crystal violet (Sigma) and scored using Image J software. Soft agar assay was carried out as previously described [8]. For the cell death assay, U373MG cells were infected with either Ad-p53 or Ad-LacZ at 6 hours after transfection of siRNA oligonucleotide. Apoptotic cells were quantified by FACS analysis as previously described [3]. Cell growth was determined by MTT assay using Cell Counting Kit-8 (Dojindo, Kumamoto, Japan) or by BrdU assay using Cell Proliferation ELISA BrdU (Roche).

Senescence-Associated β-Gal Staining

Senescence-associated (SA)–β-gal activity was detected as previously described [39].

Results

CLCA2 *Expression Is Increased during Replicative Senescence*

To investigate the genes involved in the process of cellular senescence, we compared the mRNA expression profiles of early- and late-passage (senescent) fibroblasts. Newly purchased NHDF cells were serially cultured under the conditions recommended by the distributors. Culture medium was changed every 3 days. When the cells reached 80% to 90% confluence, they were detached and plated at a density of 5×10^5 cell per 10-cm dish (approximately 30% confluence). Cell proliferation ratio of senescent fibroblast cells declined, and the cells became positive for SA-β-gal staining, which is a known senescence marker (Figure W1*A*). After passaging NHDF cells more than 30 times, they reached the senescence stage and almost stopped to grow. We conducted a cDNA microarray analysis using mRNAs from NHDF cells at the 3rd, 7th, 13th, 19th, and 26th passage levels. Through this analysis, we identified 85 genes that were increased by more than 10-fold in senescent fibroblast after the 26th passage (Table W1).

To identify novel p53 target genes, we had previously performed another mRNA expression profile analysis using U373MG p53-mutant glioblastoma cells in which wild-type p53 (Ad-p53) or LacZ (Ad-LacZ) were infected using an adenovirus system [7]. The comparison of these two data sets revealed six possible candidates that were increased by more than 10-fold in both data sets (Table W1). After performing semiquantitative reverse transcription (RT)–PCR for these six genes, we selected CLCA2 for further analysis because *CLCA2* was remarkably increased during the cellular senescence process as well as by the ectopic induction of wild-type p53 (Figures 1*A* and W1, *B* and *C*). We also confirmed the p53-mediated CLCA2 induction by quantitative RT-PCR, Northern, and Western blot analyses (Figures 1, *B* and *C*, and W2*A*). The specificity of this antibody was verified by siRNA knockdown (Figure W2, *A* and *B*).

To investigate whether CLCA2 is involved in stress-induced pathway, we analyzed the expression of *CLCA2* during oxidative stress–induced cellular senescence. We treated IMR-90 normal human diploid fibroblast cells with hydrogen peroxide (H_2O_2) and examined the expression of *CLCA2* by quantitative real-time PCR analysis (Figure 1*D*). Interestingly, $p21^{WAF1}$ and $p16^{INK4A}$ expression was increased as early as 1 or 2 days after H_2O_2 treatment, but the highest level of *CLCA2* expression was observed at 8 days in H_2O_2-treated senescent fibroblasts. These data suggest that CLCA2 is likely to play some role in the later stages of DNA damage response.

Clca5 (Mouse Homologue of Human CLCA2) Is a Target of p53

Because *Clca5* (mouse homologue of human CLCA2) was previously shown to be induced by genotoxic stress and suppress cell growth [40,41], we investigated whether *Clca5* is associated with the p53-induced senescence induction. When MEFs derived from $p53^{+/+}$ or $p53^{-/-}$ embryos were treated with oxidative stress, we found decreased staining of SA-β-gal in $p53^{-/-}$ MEF (Figure 2*A*). We also found that *Clca5* expression was induced by oxidative stress in $p53^{+/+}$ MEF but not in $p53^{-/-}$ MEF (Figure 2*B*). We then surveyed the genomic sequence of the *Clca5* gene and found three putative p53-binding sequences (p53BS 1-3) in the promoter or intron 1 region (Figure 2*C*). We subcloned a DNA fragment of 1301 base pairs, which included the three putative p53-binding sequences into pGL3 promoter vector (pGL3/p53BR; Promega). We found that cotransfection of pGL3/p53BR with wild-type p53 expression plasmid enhanced the luciferase activity by more than four-fold, whereas the base substitutions within BS1 completely diminished the luciferase activity (Figure 2*D*). Interestingly, DNA sequence of p53BS1 was highly conserved between mouse *Clca5* and human *ClCA2* (Figure W3, *A-C*). These findings indicated that Clca5/CLCA2 could be involved in the p53-induced senescence pathway.

CLCA2 Contributes to Oxidative Stress–Induced Senescence

To clarify the role of CLCA2 in genotoxic stress–induced senescence pathway, we analyzed the expression of *CLCA2* in H_2O_2-treated IMR-90 cells that were transfected with siRNA against p53 (sip53) or CLCA2 (siCLCA2-1 or siCLCA2-2). The result of quantitative real-time PCR analysis showed the drastic suppression of *CLCA2* expression by p53 knockdown to the same extent as siCLCA2 treatment (Figure 3*A*). Moreover, inhibition of CLCA2 or p53 expression significantly suppressed H_2O_2-induced cellular senescence (Figure 3*B*). We also examined whether ectopic expression of CLCA2 could induce cellular senescence. MCF7 cells were stained with SA-β-gal 3 days after introduction of CLCA2-expression plasmid. As a result, we found an

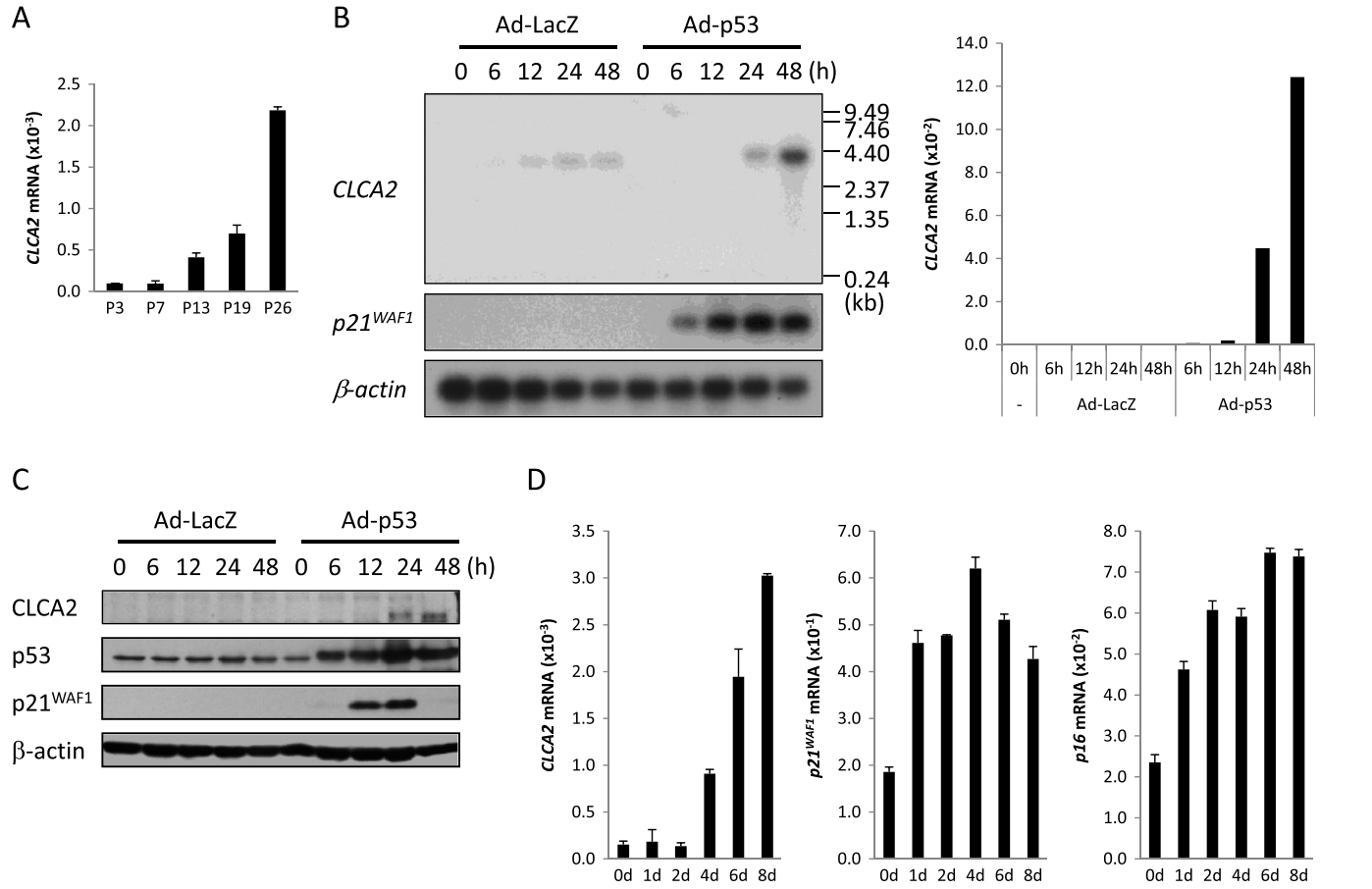

Figure 1. *CLCA2* expression is increased during replicative senescence. (A) Quantitative real-time PCR analysis of *CLCA2* mRNA in NHDF cells at indicated passage levels. *β2-Microglobulin* was used for the normalization of expression levels. (B) Northern blot and quantitative real-time PCR analysis of *CLCA2* transcript in U373MG cells at indicated times after infection with Ad-p53 or Ad-LacZ at 8 MOIs. *β-Actin* was used for the normalization of expression levels. $p21^{WAF1}$ served as a positive control. (C) Western blot analysis of CLCA2 protein in U373MG cells at indicated times after infection with Ad-p53 or Ad-LacZ at 40 MOIs. β-Actin was used for the normalization of expression levels. p53 and $p21^{WAF1}$ served as a positive control. (D) Quantitative real-time PCR analysis of *CLCA2*, $p21^{WAF1}$, and $p16^{Ink4a}$ mRNA in IMR-90 cells at the indicated days after treatment with 400 μM of H_2O_2. *β2-Microglobulin* was used for the normalization of expression levels.

increase in positive staining for SA-β-gal in cells expressing CLCA2 compared with Mock-transfected cells (Figure 3, *C* and *D*). Taken together, our findings clearly indicated that p53-CLCA2 pathway contributes to genotoxic stress–induced senescence.

Down-regulation of CLCA2 in Prostate and Colorectal Cancer

Because CLCA2 was shown to be a potential breast tumor suppressor [34], we examined the expression of *CLCA2* in various cancers using gene expression database that consists of more than 1000 cancer tissues [36,38,42–44]. The expression of *CLCA2* was remarkably decreased in breast, bladder, esophageal, lung, and prostate cancer tissues (Table 1). We performed quantitative real-time PCR analyses and found that *CLCA2* mRNA was frequently decreased in prostate and colorectal cancers (<20% of control in 9 of 10 prostate cancer tissues and in 10 of 17 colorectal cancer tissues; Figures 4*A* and W4*A*). Cellular senescence was shown to be observed in precancerous tissues and is likely to function as a barrier for malignant transformation [45]. Therefore, we investigated the expression of *CLCA2* in premalignant tissues of the prostate (prostatic intraepithelial neoplasia [PIN]). As a result, the expression of *CLCA2* in PIN is comparable with that in their corresponding normal prostate tissues but significantly higher than that in cancer tissues (Figure 4*B*).

Because expression of *CLCA2* is regulated by p53, inactivation of p53 is likely to cause the decrease of *CLCA2* expression in cancer cells. Therefore, we examined the *CLCA2* expression and the *p53* gene mutation in five prostate cancer cell lines as well as one normal prostate epithelial cell line. As a result, the expression of *CLCA2* was down-regulated in cancer cell lines compared with that of normal prostate epithelial cell line ($P < .01$), but we found no significant difference in *CLCA2* expression between wild-type and mutant p53 cell lines (Figure 4*C*; $P = .86$). These data suggested that there may be another mechanism that suppresses *CLCA2* expression in cancer cells other than p53 mutation. Because epigenetic change is one of the major causes of gene silencing in cancer tissues, we treated three prostate cancer cell lines with TSA (inhibitor of histone deacetylation) and/or 5-Aza (inhibitor of DNA methylation). We found that, after treatment, the *CLCA2* expression was partially restored in all three cell lines (Figure 4*D*), suggesting the possible role of epigenetic alteration in CLCA2 inactivation. Similarly, 5-Aza treatment increased *CLCA2* expression in two colorectal cancer cell lines among seven examined (Figure W4*B*). Nevertheless, we found that HCT116 $p53^{-/-}$ cells exhibited lower *CLCA2* expression

than HCT116 $p53^{+/+}$ cells (Figure W4*C*). In addition, cells carrying wild-type p53 exhibited relatively higher *CLCA2* expression than cells with p53 mutation, although the difference was not statistically significant ($P = .47$; Figure W4*D* and Table W2). Because p53 was frequently inactivated by various mechanisms in cancer tissues, both epigenetic alteration and p53 inactivation would play crucial roles in the deregulation of CLCA2 expression in prostate and colorectal cancer tissues.

Discussion

Here we show that *CLCA2* expression is remarkably increased during cellular senescence. Ectopic expression of CLCA2 induced senescence in cells, and knockdown of CLCA2 as well as p53 inhibited genotoxic stress–induced cellular senescence. These findings revealed that CLCA2 is a mediator of p53-induced senescence.

We have previously demonstrated the distinct mechanisms by which p53 determined cell fate through the induction of different sets of its target genes. At an early time point after repairable DNA damage, p53 induces $p21^{WAF1}$ and p53R2, which cooperatively modulate cell survival through the induction of cell cycle arrest and subsequent repair of damaged DNA [4]. However, when DNA damage is too severe to be repaired, specifically activated p53 induces genes such as *p53AIP1*, a crucial mediator of apoptotic pathway, to eliminate the damaged cells [8]. Because senescence is also an irreversible process like apoptosis, our finding suggested that p53 regulates cell fate by inducing senescence associate gene(s) when cells are severely damaged. Actually, CLCA2 expression was peaked at a later time point during replicative senescence compared with $p16^{Ink4a}$ and $p21^{WAF1}$, suggesting the activation of CLCA2 in the aging tissues. Because most prostate cancer affects elderly men, decreased expression of CLCA2 due to epigenetic alteration or p53 inactivation would play an important role in prostate carcinogenesis.

Walia et al. reported that CLCA2 regulates intracellular pH. Under physiological conditions, the ion channels maintain the body pH within a range of 7.35 to 7.45. However, the pH of tumor cells was found to be neutral or alkaline [46]. Higher pH was associated with the apoptosis resistance and the invasive property of tumor cells, and inhibition of the Na(+)/H(+) exchanger isoform 1 (NHE1) induced apoptosis in cancer cells [47]. Conversely, aging caused the change of the composition and function of cell membranes and subsequently decreased the pH [48]. Degenerative neural diseases such as Parkinson disease and Alzheimer disease indicate a decreased pH in cells and tissues [49]. Thus, intracellular pH is strongly associated with oncogenic and senescence phenotype. Taken together, CLCA2

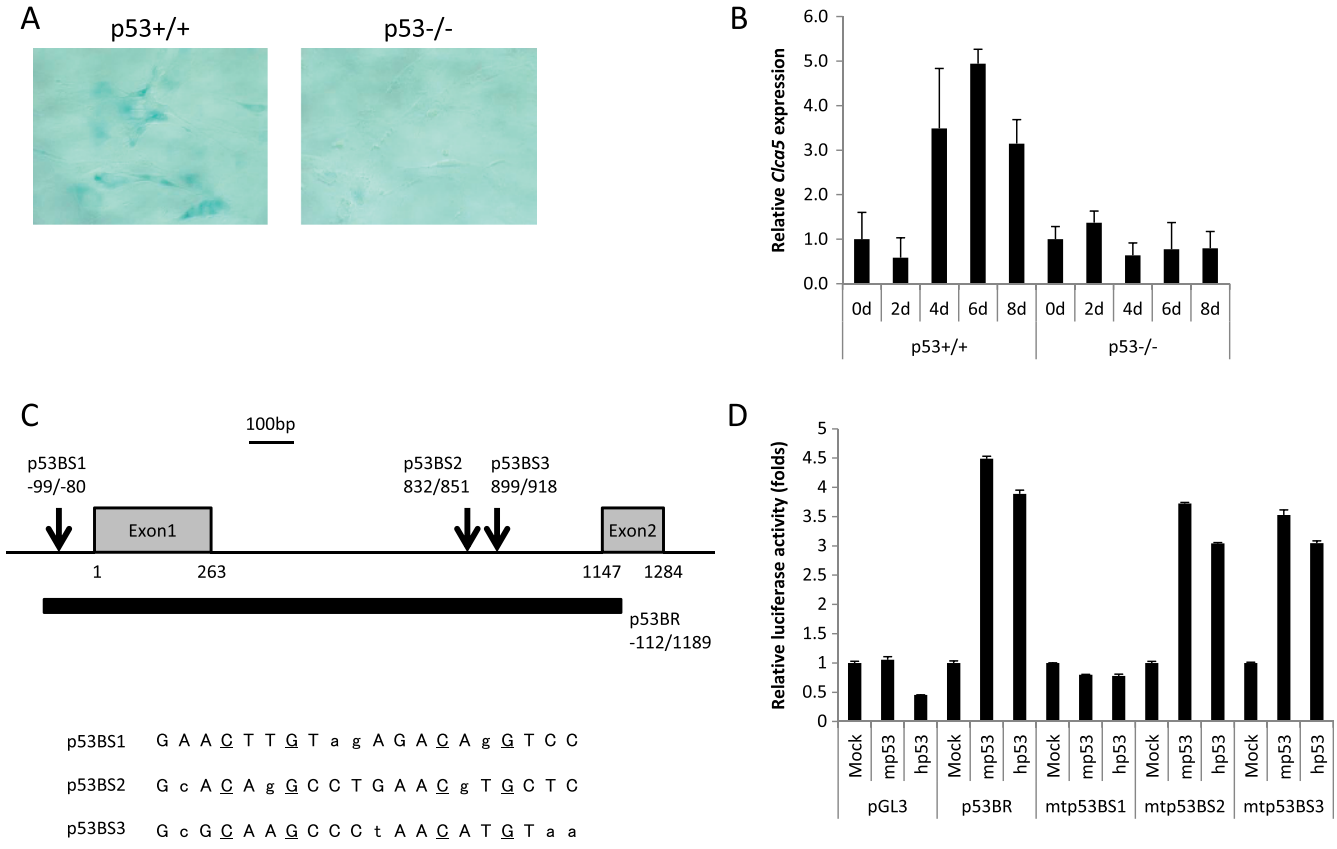

Figure 2. *Clca5* (mouse homologue of human *CLCA2*) is a target of p53. (A, B) $p53^{+/+}$ and $p53^{-/-}$ MEFs were treated with 100 μM (A) or 150 μM (B) of H_2O_2. (A) At 6 days after treatment, the cells were subjected to SA-β-gal staining. (B) Quantitative real-time PCR analysis of *Clca5* mRNA at indicated days after treatment. *β-Actin* was used for the normalization of expression levels. (C) Genomic structure of the mouse *Clca5* gene. Gray boxes indicate the locations and relative sizes of the two exons. Arrows indicate the locations of potential p53-binding sites (p53BS1-3) in a p53-binding region (p53BR). Identical nucleotides to the consensus sequence are written in capital letters. The underlined nucleotides were substituted for thymine to examine the specificity of each p53-binding site. (D) Results of luciferase assay of p53BR with or without substitutions at either of the p53BS fragments are shown. Luciferase activity is indicated relative to the activity of mock vector with SDs ($n = 2$).

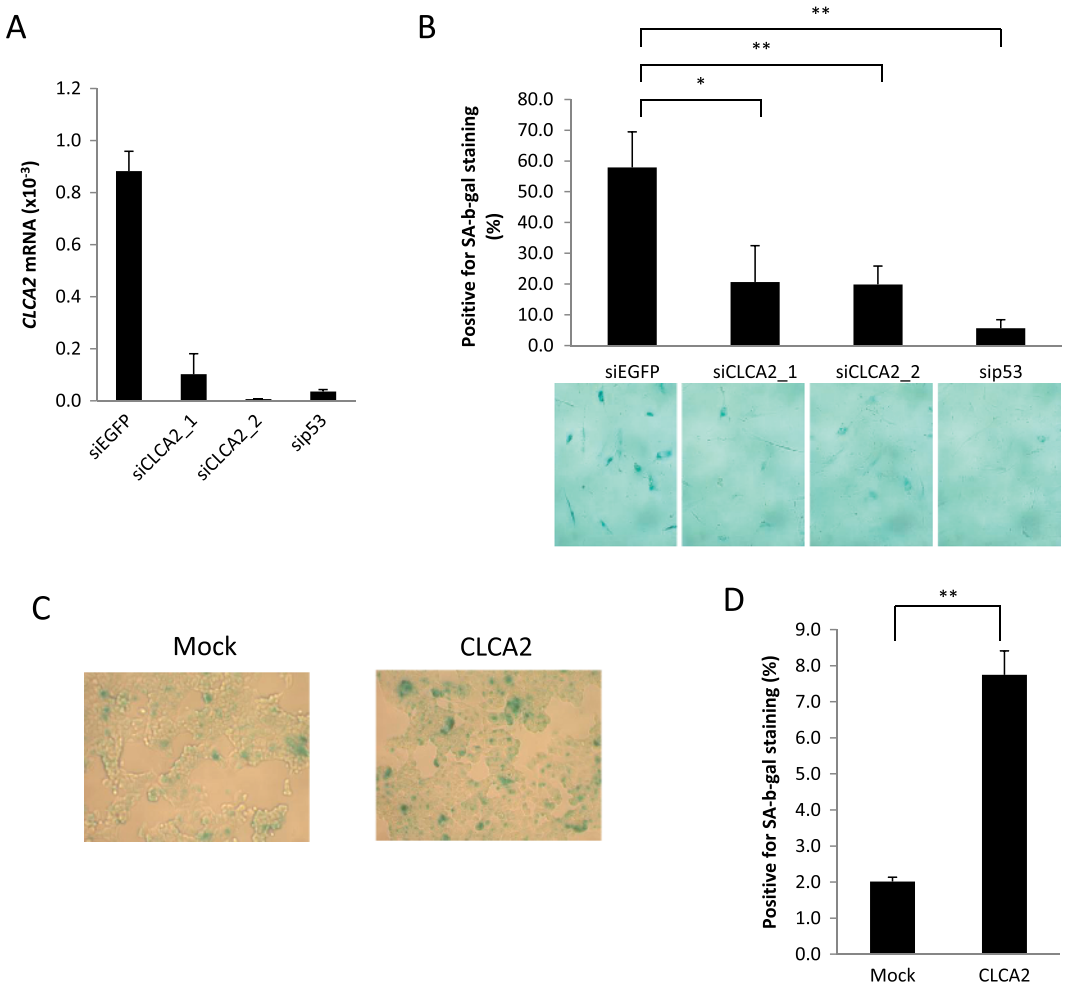

Figure 3. CLCA2 is a key mediator of oxidative stress–induced senescence. (A, B) IMR-90 cells were transfected with siRNA oligonucleotides designed to suppress the expression of *CLCA2* or p53 at 7 hours before treatment with 400 μM of H_2O_2. siEGFP was used as a control. At 8 days after treatment, the cells were subjected to quantitative real-time PCR analysis of *CLCA2* mRNA (A) and SA-β-gal staining (B). *β2-Microglobulin* was used for the normalization of expression levels. The proportion of cells positive for SA-β-gal staining is indicated (B, upper panels). The representative images of cells are shown (B, lower panels). Asterisks indicate *P* value obtained by Student's *t* test: $*P < .05$ and $**P < .01$. (C, D) MCF7 cells were transfected with CLCA2 expression plasmid. (C) After 3 days, the cells were subjected to SA-β-gal staining. (D) The proportion of cells positive for SA-β-gal staining is indicated. Asterisk indicates *P* value obtained by Student's *t* test: $**P < .01$.

could function as a barrier for malignant transformation by inducing cellular senescence and tumor regression through the regulation of intracellular pH.

N-terminal CLCA2 was shown to be cleaved and secreted into the culture medium [50]. Although several studies indicated the growth suppressive effect of membrane-localized CLCA2, the role of soluble CLCA2 was not well characterized. The physiological significance of processing at its extracellular domain varies among substrates proteins. Tumor necrosis factor α is cleaved by TACE and exhibits strong systemic effects [51]. In contrast, soluble MICA blocks natural killer cell activity [52], whereas membrane-bound MICA stimulates immune response mediated by natural killer cell [53]. E-cadherin is cleaved by metalloproteinase and a residual membrane-tethered product is degraded by intracellular proteolytic pathway [54]. Because senescent human fibroblasts were shown to stimulate proliferation of epithelial cells *in vitro* and *in vivo* [55], soluble CLCA2 secreted by the senescence-activated fibroblasts might exhibit growth-promoting activity in contrast to the membrane-localized CLCA2. We would like to analyze the role of membrane-localized and soluble CLCA2 on the regulation of cellular senescence pathway in the future study. Many organ-specific serum biomarkers for aging such as N-telopeptide of type I collagen and MT1-MMP for bone resorption [56], CD4/CD8 ratio for immune system, albumin, and

Table 1. Decreased Expression of *CLCA2* in Cancer Tissues Examined by cDNA Microarray Analyses.

Cancer Tissues	Suppression of *CLCA2* (<1/3), *n* (%)	Total Samples (*n*)	References
Lung cancer (SCLC)	7 (100)	7	Taniwaki et al. [36]
Prostate cancer	21 (81)	26	Ashida et al. [38]
Esophageal cancer	10 (53)	19	Yamabuki et al. [42]
Breast cancer	30 (46)	66	Nishidate et al. [44]
Bladder cancer	9 (28)	32	Takata et al. [43]

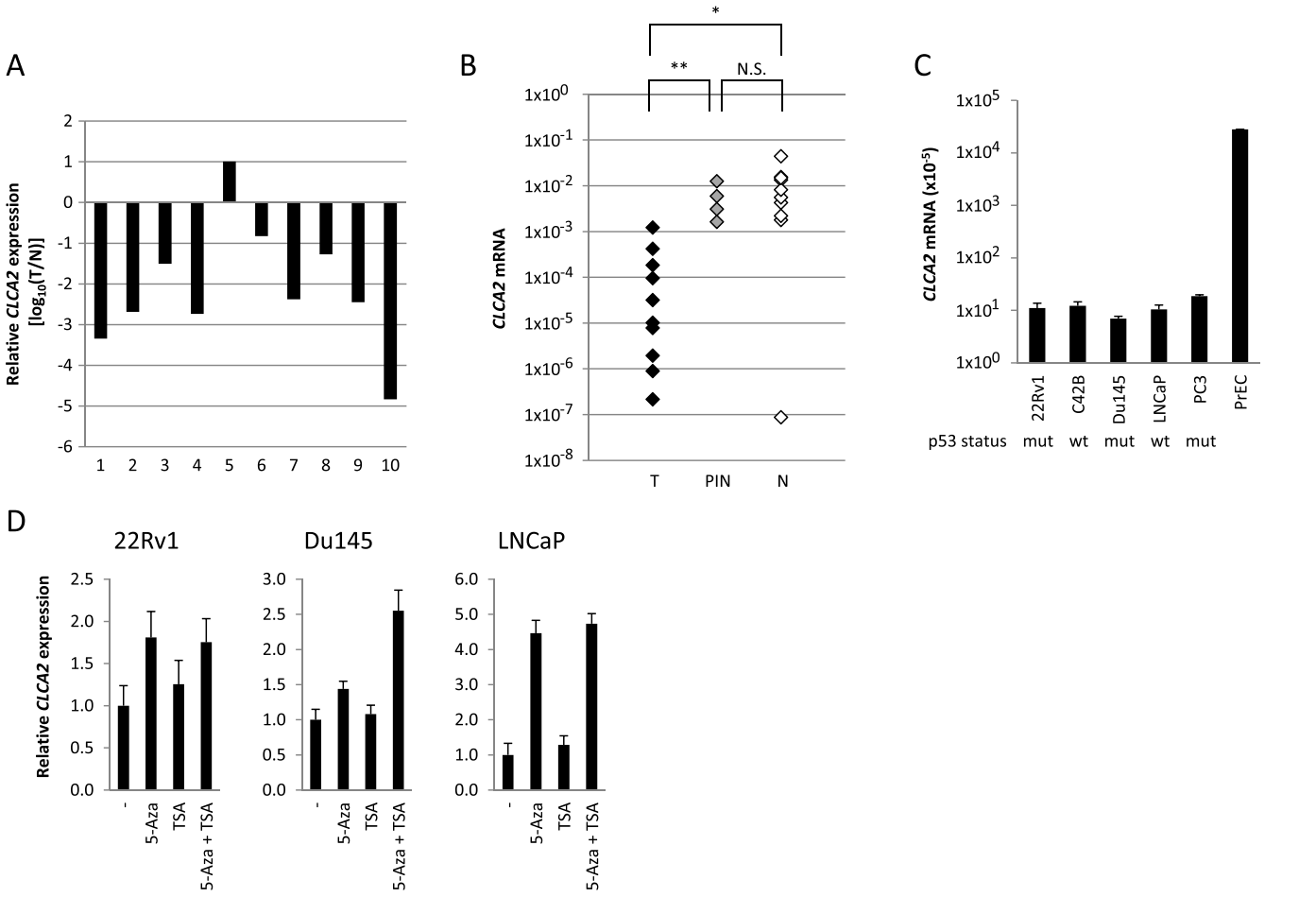

Figure 4. Down-regulation of CLCA2 in prostate cancer. (A) Relative *CLCA2* expression in prostate cancer tissues compared with normal tissues was examined by quantitative real-time PCR analysis. *β-Actin* was used for the normalization of expression levels. (B) *CLCA2* expressions in prostate cancer tissues, PIN, and normal tissues were examined by quantitative real-time PCR analysis. *β-Actin* was used for the normalization of expression levels. (C) *CLCA2* expressions in prostate cancer cell lines were examined by quantitative real-time PCR analysis. *β2-Microglobulin* was used for the normalization of expression levels. (D) Three prostate cancer cell lines were treated with 5 μM of 5-Aza and/or 0.5 μM of TSA. *CLCA2* expressions were examined by quantitative real-time PCR analysis. *β2-Microglobulin* was used for the normalization of expression levels. Asterisks indicate *P* value obtained by Student's *t* test: $*P < .05$, $**P < .01$, and N.S. (not statistically significant).

growth hormone for nutrition [57] are clinically valuable [58]. Telomere length is a good marker for biologic aging [59], but serum biomarkers of human aging have not yet been clinically validated. Because CLCA2 was increased in response to genotoxic stress as well as replicative senescence, serum CLCA2 would be a good biomarker for aging. Although we have not yet been able to establish an ELISA test to detect soluble CLCA2 owing to the high background of antibody, we would like to investigate the role of soluble CLCA2 as a senescence biomarker in the future.

Although further functional analyses, especially for the role of the cleaved N-terminal fragment, are essential to fully elucidate the role of CLCA2 in senescence and carcinogenesis, we believe that our findings may lead to the development of a novel cancer therapy by reactivating CLCA2 signaling.

Acknowledgments

The authors thank T. Katagiri for helpful discussions and K. Makino for technical assistance.

References

[1] Soussi T, Asselain B, Hamroun D, Kato S, Ishioka C, Claustres M, and Beroud C (2006). Meta-analysis of the p53 mutation database for mutant p53 biological activity reveals a methodologic bias in mutation detection. *Clin Cancer Res* **12**, 62–69.

[2] Vogelstein B, Lane D, and Levine AJ (2000). Surfing the p53 network. *Nature* **408**, 307–310.

[3] Matsuda K, Yoshida K, Taya Y, Nakamura K, Nakamura Y, and Arakawa H (2002). $p53^{AIP1}$ regulates the mitochondrial apoptotic pathway. *Cancer Res* **62**, 2883–2889.

[4] Tanaka H, Arakawa H, Yamaguchi T, Shiraishi K, Fukuda S, Matsui K, Takei Y, and Nakamura Y (2000). A ribonucleotide reductase gene involved in a p53-dependent cell-cycle checkpoint for DNA damage. *Nature* **404**, 42–49.

[5] el-Deiry WS (1998). Regulation of p53 downstream genes. *Semin Cancer Biol* **8**, 345–357.

[6] Nakamura Y (2004). Isolation of p53-target genes and their functional analysis. *Cancer Sci* **95**, 7–11.

[7] Tanikawa C, Furukawa Y, Yoshida N, Arakawa H, Nakamura Y, and Matsuda K (2009). XEDAR as a putative colorectal tumor suppressor that mediates p53-regulated anoikis pathway. *Oncogene* **28**, 3081–3092.

[8] Oda K, Arakawa H, Tanaka T, Matsuda K, Tanikawa C, Mori T, Nishimori H, Tamai K, Tokino T, Nakamura Y, et al. (2000). $p53^{AIP1}$, a potential mediator

of p53-dependent apoptosis, and its regulation by Ser-46–phosphorylated p53. *Cell* **102**, 849–862.

[9] Tanikawa C, Matsuda K, Fukuda S, Nakamura Y, and Arakawa H (2003). $p53^{RDL1}$ regulates p53-dependent apoptosis. *Nat Cell Biol* **5**, 216–223.

[10] Tanikawa C, Ueda K, Nakagawa H, Yoshida N, Nakamura Y, and Matsuda K (2009). Regulation of protein citrullination through p53/PADI4 network in DNA damage response. *Cancer Res* **69**, 8761–8769.

[11] Tanikawa C, Ri C, Kumar V, Nakamura Y, and Matsuda K (2010). Cross-talk of EDA-A2/XEDAR in the p53 signaling pathway. *Mol Cancer Res* **8**, 855–863.

[12] Kidokoro T, Tanikawa C, Furukawa Y, Katagiri T, Nakamura Y, and Matsuda K (2008). CDC20, a potential cancer therapeutic target, is negatively regulated by p53. *Oncogene* **27**, 1562–1571.

[13] Tanikawa C, Espinosa M, Suzuki A, Masuda K, Yamamoto K, Tsuchiya E, Ueda K, Daigo Y, Nakamura Y, and Matsuda K (2012). Regulation of histone modification and chromatin structure by the p53-PADI4 pathway. *Nat Commun* **3**, 676.

[14] Schmitt CA, Fridman JS, Yang M, Lee S, Baranov E, Hoffman RM, and Lowe SW (2002). A senescence program controlled by p53 and $p16^{INK4a}$ contributes to the outcome of cancer therapy. *Cell* **109**, 335–346.

[15] Agger K, Cloos PA, Rudkjaer L, Williams K, Andersen G, Christensen J, and Helin K (2009). The H3K27me3 demethylase JMJD3 contributes to the activation of the INK4A-ARF locus in response to oncogene- and stress-induced senescence. *Genes Dev* **23**, 1171–1176.

[16] Zindy F, Quelle DE, Roussel MF, and Sherr CJ (1997). Expression of the $p16^{INK4a}$ tumor suppressor *versus* other INK4 family members during mouse development and aging. *Oncogene* **15**, 203–211.

[17] Ressler S, Bartkova J, Niederegger H, Bartek J, Scharffetter-Kochanek K, Jansen-Durr P, and Wlaschek M (2006). $p16^{INK4A}$ is a robust *in vivo* biomarker of cellular aging in human skin. *Aging Cell* **5**, 379–389.

[18] Wu J, Xue L, Weng M, Sun Y, Zhang Z, Wang W, and Tong T (2007). Sp1 is essential for p16 expression in human diploid fibroblasts during senescence. *PLoS One* **2**, e164.

[19] Quereda V, Martinalbo J, Dubus P, Carnero A, and Malumbres M (2007). Genetic cooperation between $p21^{Cip1}$ and INK4 inhibitors in cellular senescence and tumor suppression. *Oncogene* **26**, 7665–7674.

[20] Ksiazek K, Piwocka K, Brzezinska A, Sikora E, Zabel M, Breborowicz A, Jorres A, and Witowski J (2006). Early loss of proliferative potential of human peritoneal mesothelial cells in culture: the role of $p16^{INK4a}$-mediated premature senescence. *J Appl Physiol* **100**, 988–995.

[21] Gil J and Peters G (2006). Regulation of the INK4b-ARF-INK4a tumour suppressor locus: all for one or one for all. *Nat Rev Mol Cell Biol* **7**, 667–677.

[22] Romagosa C, Simonetti S, Lopez-Vicente L, Mazo A, Lleonart ME, Castellvi J, and Ramon y Cajal S (2011). $p16^{Ink4a}$ overexpression in cancer: a tumor suppressor gene associated with senescence and high-grade tumors. *Oncogene* **30**, 2087–2097.

[23] Harvey M, Sands AT, Weiss RS, Hegi ME, Wiseman RW, Pantazis P, Giovanella BC, Tainsky MA, Bradley A, and Donehower LA (1993). *In vitro* growth characteristics of embryo fibroblasts isolated from p53-deficient mice. *Oncogene* **8**, 2457–2467.

[24] Xue W, Zender L, Miething C, Dickins RA, Hernando E, Krizhanovsky V, Cordon-Cardo C, and Lowe SW (2007). Senescence and tumour clearance is triggered by p53 restoration in murine liver carcinomas. *Nature* **445**, 656–660.

[25] Tyner SD, Venkatachalam S, Choi J, Jones S, Ghebranious N, Igelmann H, Lu X, Soron G, Cooper B, Brayton C, et al. (2002). p53 mutant mice that display early ageing-associated phenotypes. *Nature* **415**, 45–53.

[26] Chen Z, Trotman LC, Shaffer D, Lin HK, Dotan ZA, Niki M, Koutcher JA, Scher HI, Ludwig T, Gerald W, et al. (2005). Crucial role of p53-dependent cellular senescence in suppression of Pten-deficient tumorigenesis. *Nature* **436**, 725–730.

[27] Bartkova J, Rezaei N, Liontos M, Karakaidos P, Kletsas D, Issaeva N, Vassiliou LV, Kolettas E, Niforou K, Zoumpourlis VC, et al. (2006). Oncogene-induced senescence is part of the tumorigenesis barrier imposed by DNA damage checkpoints. *Nature* **444**, 633–637.

[28] Collado M, Gil J, Efeyan A, Guerra C, Schuhmacher AJ, Barradas M, Benguria A, Zaballos A, Flores JM, Barbacid M, et al. (2005). Tumour biology: senescence in premalignant tumours. *Nature* **436**, 642.

[29] Campisi J (2005). Senescent cells, tumor suppression, and organismal aging: good citizens, bad neighbors. *Cell* **120**, 513–522.

[30] Herbig U, Jobling WA, Chen BP, Chen DJ, and Sedivy JM (2004). Telomere shortening triggers senescence of human cells through a pathway involving ATM, p53, and p21(CIP1), but not p16(INK4a). *Mol Cell* **14**, 501–513.

[31] Wang YA, Elson A, and Leder P (1997). Loss of p21 increases sensitivity to ionizing radiation and delays the onset of lymphoma in atm-deficient mice. *Proc Natl Acad Sci USA* **94**, 14590–14595.

[32] Walia V, Ding M, Kumar S, Nie D, Premkumar LS, and Elble RC (2009). hCLCA2 is a p53-inducible inhibitor of breast cancer cell proliferation. *Cancer Res* **69**, 6624–6632.

[33] Gruber AD and Pauli BU (1999). Tumorigenicity of human breast cancer is associated with loss of the Ca^{2+}-activated chloride channel CLCA2. *Cancer Res* **59**, 5488–5491.

[34] Li X, Cowell JK, and Sossey-Alaoui K (2004). CLCA2 tumour suppressor gene in 1p31 is epigenetically regulated in breast cancer. *Oncogene* **23**, 1474–1480.

[35] Rovillain E, Mansfield L, Caetano C, Alvarez-Fernandez M, Caballero OL, Medema RH, Hummerich H, and Jat PS (2011). Activation of nuclear factor-κ B signalling promotes cellular senescence. *Oncogene* **30**, 2356–2366.

[36] Taniwaki M, Daigo Y, Ishikawa N, Takano A, Tsunoda T, Yasui W, Inai K, Kohno N, and Nakamura Y (2006). Gene expression profiles of small-cell lung cancers: molecular signatures of lung cancer. *Int J Oncol* **29**, 567–575.

[37] Tsukada T, Tomooka Y, Takai S, Ueda Y, Nishikawa S, Yagi T, Tokunaga T, Takeda N, Suda Y, Abe S, et al. (1993). Enhanced proliferative potential in culture of cells from p53-deficient mice. *Oncogene* **8**, 3313–3322.

[38] Ashida S, Nakagawa H, Katagiri T, Furihata M, Iiizumi M, Anazawa Y, Tsunoda T, Takata R, Kasahara K, Miki T, et al. (2004). Molecular features of the transition from prostatic intraepithelial neoplasia (PIN) to prostate cancer: genome-wide gene-expression profiles of prostate cancers and PINs. *Cancer Res* **64**, 5963–5972.

[39] Dimri GP, Lee X, Basile G, Acosta M, Scott G, Roskelley C, Medrano EE, Linskens M, Rubelj I, Pereira-Smith O, et al. (1995). A biomarker that identifies senescent human cells in culture and in aging skin *in vivo*. *Proc Natl Acad Sci USA* **92**, 9363–9367.

[40] Beckley JR, Pauli BU, and Elble RC (2004). Re-expression of detachment-inducible chloride channel mCLCA5 suppresses growth of metastatic breast cancer cells. *J Biol Chem* **279**, 41634–41641.

[41] Elble RC and Pauli BU (2001). Tumor suppression by a proapoptotic calcium-activated chloride channel in mammary epithelium. *J Biol Chem* **276**, 40510–40517.

[42] Yamabuki T, Daigo Y, Kato T, Hayama S, Tsunoda T, Miyamoto M, Ito T, Fujita M, Hosokawa M, Kondo S, et al. (2006). Genome-wide gene expression profile analysis of esophageal squamous cell carcinomas. *Int J Oncol* **28**, 1375–1384.

[43] Takata R, Katagiri T, Kanehira M, Tsunoda T, Shuin T, Miki T, Namiki M, Kohri K, Matsushita Y, Fujioka T, et al. (2005). Predicting response to methotrexate, vinblastine, doxorubicin, and cisplatin neoadjuvant chemotherapy for bladder cancers through genome-wide gene expression profiling. *Clin Cancer Res* **11**, 2625–2636.

[44] Nishidate T, Katagiri T, Lin ML, Mano Y, Miki Y, Kasumi F, Yoshimoto M, Tsunoda T, Hirata K, and Nakamura Y (2004). Genome-wide gene-expression profiles of breast-cancer cells purified with laser microbeam microdissection: identification of genes associated with progression and metastasis. *Int J Oncol* **25**, 797–819.

[45] Majumder PK, Grisanzio C, O'Connell F, Barry M, Brito JM, Xu Q, Guney I, Berger R, Herman P, Bikoff R, et al. (2008). A prostatic intraepithelial neoplasia-dependent p27 Kip1 checkpoint induces senescence and inhibits cell proliferation and cancer progression. *Cancer Cell* **14**, 146–155.

[46] Reshkin SJ, Bellizzi A, Albarani V, Guerra L, Tommasino M, Paradiso A, and Casavola V (2000). Phosphoinositide 3-kinase is involved in the tumor-specific activation of human breast cancer cell Na(+)/H(+) exchange, motility, and invasion induced by serum deprivation. *J Biol Chem* **275**, 5361–5369.

[47] Rich IN, Worthington-White D, Garden OA, and Musk P (2000). Apoptosis of leukemic cells accompanies reduction in intracellular pH after targeted inhibition of the Na(+)/H(+) exchanger. *Blood* **95**, 1427–1434.

[48] Marinho CF, Costa-Maia J, Pinto-de-Barros J, and Oliveira CR (1997). Correlation between human platelet cytoplasmic membrane outer leaflet fluidity, Na^+/H^+ exchanger activity and aging. *Eur Arch Psychiatry Clin Neurosci* **247**, 275–277.

[49] Xiong Z-G, Pignataro G, Li M, Chang S-Y, and Simon RP (2008). Acid-sensing ion channels (ASICs) as pharmacological targets for neurodegenerative diseases. *Curr Opin Pharmacol* **8**, 25–32.

[50] Elble RC, Walia V, Cheng HC, Connon CJ, Mundhenk L, Gruber AD, and Pauli BU (2006). The putative chloride channel hCLCA2 has a single C-terminal transmembrane segment. *J Biol Chem* **281**, 29448–29454.

[51] Kriegler M, Perez C, DeFay K, Albert I, and Lu SD (1988). A novel form of TNF/cachectin is a cell surface cytotoxic transmembrane protein: ramifications for the complex physiology of TNF. *Cell* **53**, 45–53.

[52] Bauer S, Groh V, Wu J, Steinle A, Phillips JH, Lanier LL, and Spies T (1999). Activation of NK cells and T cells by NKG2D, a receptor for stress-inducible MICA. *Science* **285**, 727–729.

[53] Groh V, Wu J, Yee C, and Spies T (2002). Tumour-derived soluble MIC ligands impair expression of NKG2D and T-cell activation. *Nature* **419**, 734–738.

[54] Ito K, Okamoto I, Araki N, Kawano Y, Nakao M, Fujiyama S, Tomita K, Mimori T, and Saya H (1999). Calcium influx triggers the sequential proteolysis of extracellular and cytoplasmic domains of E-cadherin, leading to loss of β-catenin from cell-cell contacts. *Oncogene* **18**, 7080–7090.

[55] Krtolica A, Parrinello S, Lockett S, Desprez PY, and Campisi J (2001). Senescent fibroblasts promote epithelial cell growth and tumorigenesis: a link between cancer and aging. *Proc Natl Acad Sci USA* **98**, 12072–12077.

[56] Ren XH, Peng XD, Wu XP, Liao EY, and Sun ZQ (2008). Association between serum soluble membrane type matrix metalloproteinase-1 (MT1-MMP) levels and bone mineral density, and biochemical markers in postmenopausal women. *Clin Chim Acta* **390**, 44–48.

[57] Yang SC, Chiang CK, Hsu SP, and Hung KY (2008). Relationship between interdialytic weight gain and nutritional markers in younger and older hemodialysis patients. *J Ren Nutr* **18**, 210–222.

[58] Thompson HJ and Voss JG (2009). Health- and disease-related biomarkers in aging research. *Res Gerontol Nurs* **2**, 137–148.

[59] Bekaert S, De Meyer T, and Van Oostveldt P (2005). Telomere attrition as ageing biomarker. *Anticancer Res* **25**, 3011–3021.

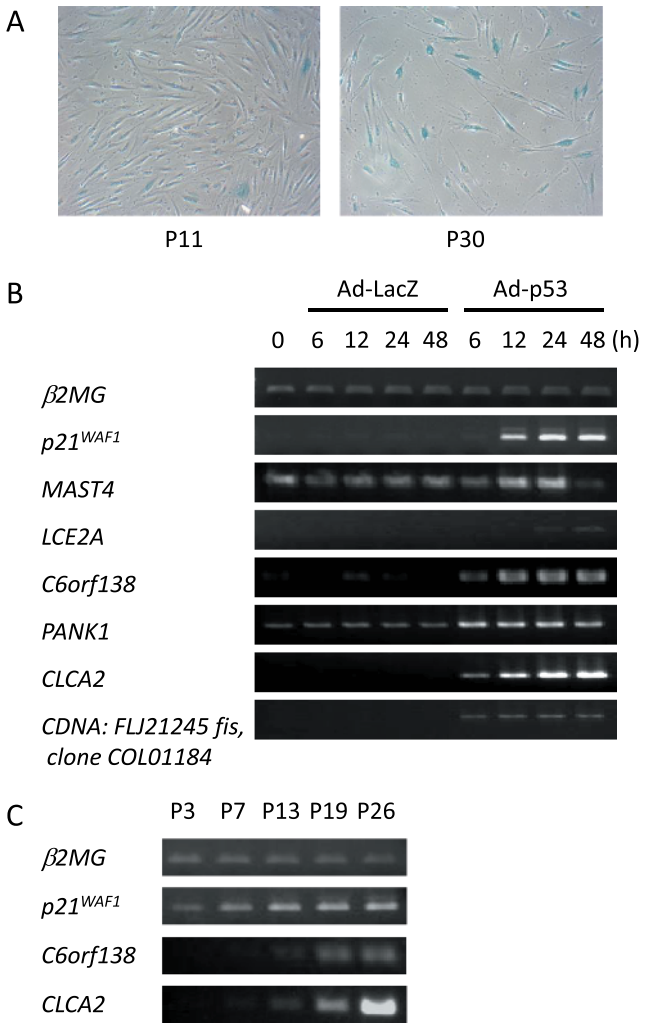

Figure W1. Replicative senescence in late-passage fibroblast. (A) After 30 times of passage, the cells were subjected to SA-β-gal staining. (B) RT-PCR analysis of six candidate mRNAs in U373MG cells at indicated times after infection with Ad-p53 or Ad-LacZ. *β2-Microglobulin* was used for the normalization of expression levels. *p21*^{WAF1} served as a positive control. (C) RT-PCR analysis of *C6orf138* and *CLCA2* mRNAs in NHDF cells at indicated passage levels. *β2-Microglobulin* was used for the normalization of expression levels. *p21*^{WAF1} served as a positive control.

Table W1. List of 85 Senescence-Associated Genes.

Gene	P26/P3	p53 Induction
MAST4	>50	++
RGS4	>50	
PPP4R4	>50	
ZNF367	>50	
SORT1	>50	
SYPL2	>50	
LCE2A	>50	++
MOSC1	>50	
TOMM40L	>50	
CDNA FLJ32320 fis	>50	
SDPR	>50	
PPFIA2	>50	
KIAA1147	>50	
C6orf138	>50	++
DSCC1	>50	
POLR3G	>50	
ETV4	>50	
PARG	>50	
SIGLEC15	>50	
Clone IMAGE:35527	>50	
LEPR	>50	
RBM24	>50	
BRI3BP	>50	
ANXA1	>50	
HSFE-1	>50	
Clone 23555	>50	
CCIN	>50	
CACNA1H	>50	
SLC7A14	>50	
KLRF1	>50	+
PANK1	>50	++
ENPP5	>50	
CPEB2	>50	
C11orf41	>50	
cDNA DKFZp686O 1044	>50	
TFDP1	>50	
RASD1	>50	
NAP1L2	>50	
DHRS12	>50	
EIF2C1	>50	
SLC7A14	>50	
CLCA2	>50	++
CYP3A5	>50	

Table W1. (*continued*).

Gene	P26/P3	p53 Induction
RNLS	>50	
MAST4	41.74	
SFRP4	41.67	
RGS2	40.24	
DTL	39.38	
NPTX1	30.78	
INA	29.34	
NAT8L	28.66	+
MMP1	28.28	
DBNDD1	24.25	
CCND1	22.55	
ATP8B4	22.11	
GLTPD1	22.02	
MET	21.58	
CCND1	20.73	
MFAP1	20.20	
CCND2	18.71	
C9orf57	18.21	
FNDC5	16.78	
PHLDA1	15.91	
CIT	15.55	
SLC1A2	15.32	
KLHDC9	14.87	
TOR1AIP1	14.55	
IFIT2	14.42	
ENY2	14.26	
RNF219	13.97	
CDNA: FLJ21245 fis	13.40	++
PRKG2	12.32	
TNIK	12.06	
APBA1	11.76	
TMEM158	11.58	+
E2F7	11.33	+
CNTN3	10.96	
CYYR1	10.93	
SLC35A3	10.77	
GPR68	10.76	
SYNM	10.63	
ITGA6	10.56	
VWF	10.54	
PLCB1	10.38	
CENPQ	10.19	

"+" indicates more than 5-fold induction at 24 or 48 hours after infection with Ad-p53; "++," more than 10-fold induction at 24 or 48 hours after infection with Ad-p53.

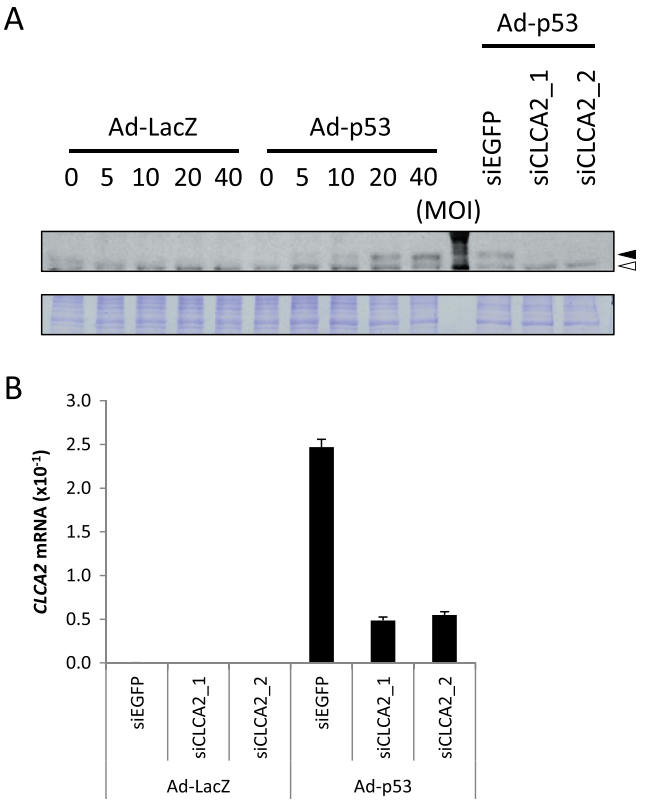

Figure W2. Ectopic expression of p53 induced CLCA2 protein. (A) Western blot analysis of CLCA2 protein in U373MG cells at 48 hours after infection with Ad-p53 or Ad-LacZ at indicated doze. CBB staining was used for the normalization protein loading. siCLCA2_1, siCLCA2_2, or siEGFP was transfected at 7 hours before adenovirus infection at 20 MOI. Black arrowhead indicates CLCA2 protein; open arrowhead, nonspecific band. (B) Quantitative RT-PCR analysis of CLCA2 in U373MG cells 48 hours after infection with Ad-LacZ or Ad-p53 at 20 MOI. siCLCA2_1, siCLCA2_2, or siEGFP was transfected 7 hours before adenovirus infection.

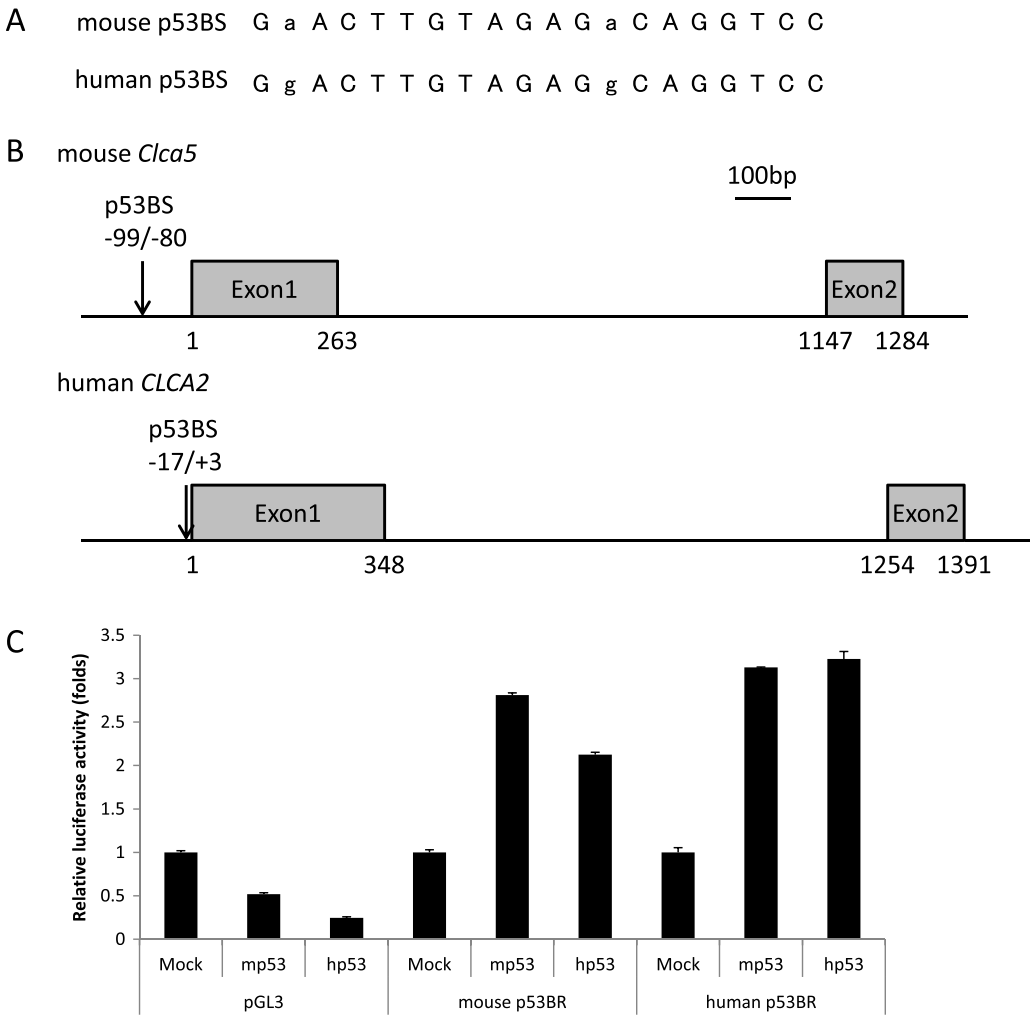

Figure W3. Comparison of mouse *Clca5* and human CLCA2. (A) Alignment of mouse p53BS and human p53BS. Nucleotides conserved between human and mouse are written in capital letters. (B) Genomic structures of the mouse *Clca5* and human *CLCA2* genes. Gray boxes indicate the locations and relative sizes of the two exons. Arrows indicate the locations of potential p53-binding sites. (C) Results of luciferase assay of p53BR are shown. Luciferase activity is indicated relative to the activity of mock vector with SDs ($n = 2$).

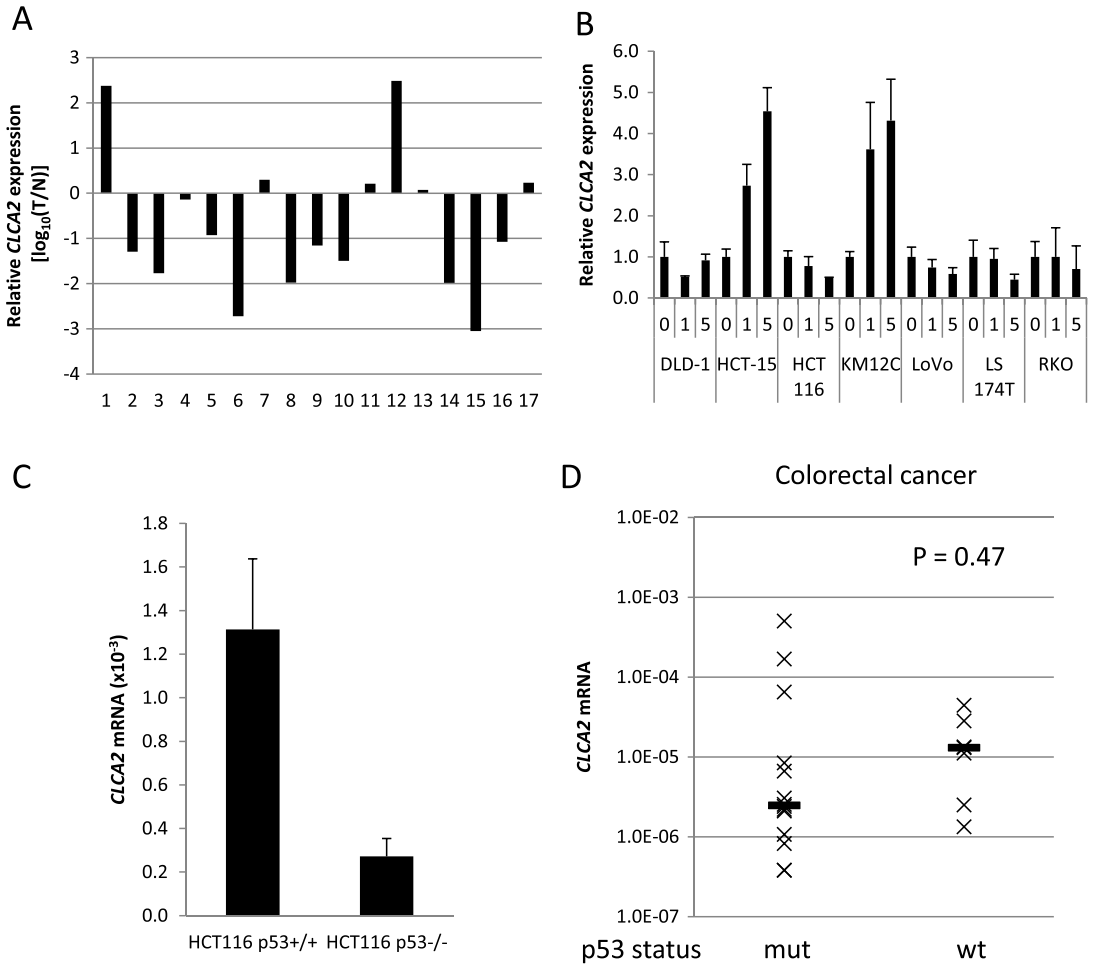

Figure W4. Suppression of *CLCA2* expression in colorectal cancer tissues. (A) Relative *CLCA2* expressions in colorectal cancer tissues compared with normal tissues were examined by quantitative real-time PCR analysis. *β-Actin* was used for the normalization of expression levels. (B) Seven colorectal cancer cell lines were treated with 1 or 5 μM of 5-Aza. *CLCA2* expressions were examined by quantitative real-time PCR analysis. *β2-Microglobulin* was used for the normalization of expression levels. (C) *CLCA2* expressions were examined by quantitative real-time PCR analysis. *β2-Microglobulin* was used for the normalization of expression levels. (D) *CLCA2* expressions were examined by quantitative real-time PCR analysis in 21 colorectal cancer cell lines. *β2-Microglobulin* was used for the normalization of expression levels. Student's *t* test was applied for comparing the *CLCA2* expressions in p53 mutant cell lines with those in p53 wild-type cell lines.

Table W2. List of Cancer Cell Lines.

No.	Colorectal Cancer Cell Lines
1	DLD-1
2	HCT-15
3	HT-29
4	KM12C
5	KM12SM
6	NCI-H508
7	NCI-H684
8	NCI-H716
9	SNU-C2A
10	SNU C5
11	SW480
12	SW620
13	SW948
14	WiDr
15	HCT 116
16	LoVo
17	LS 174T
18	NCI-H498
19	RKO
20	SNU C4
21	SW48

Table W3. Sequences of Primers and RNA Nucleotides.

	Sense	Antisense
siRNA oligonucleotides		
siCLCA2_1	GGAAUUUACUCGAGGUAUUTT	AAUACCUCGAGUAAAUUCCTT
siCLCA2_2	GAUGAAUGCUCCAAGGAAATT	UUUCCUUGGAGCAUUCAUCTT
sip53	GACUCCAGUGGUAAUCUACTT	GUAGAUUACCACUGGAGUCTT
siEGFP	GCAGCACGACUUCUUCAAGTT	CUUGAAGAAGUCGUGCUGCTT
	Forward	**Reverse**
Quantitative real-time PCR (SYBR Green I Master)		
CLCA2	ATACCTGCCACATGGAAAGC	CCTCTTTTCCACACCCTCTG
$p21^{WAF1}$	AAGATCAGCCGGCGTTTG	GACCTGTCACTGTCTTGTACCC
β2-Microglobulin	TCTCTCTTTCTGGCCTGGAG	AATGTCGGATGGATGAAACC
Clca5 (mouse)	CCGAGTGGTCTGCTTAGTGA	TACAGTTCGGCTGCTTGTTG
β-Actin (mouse)	CTAAGGCCAACCGTGAAAAG	ACCAGAGGCATACAGGGACA
p16	AGCATGGAGCCTTCGGCTGA	CCATCATCATGACCTGGATCG
Quantitative real-time PCR (Probe Master)		
CLCA2 no. 21	AGAAGAGGTCAGCAGGGAGA	CTCTTGATGGAGAAAGGATTAAAGA
β-Actin no. 55	TAGGAGGGCTGGCAACTTAG	CCAAGATGTTGATGTTGGATAAGA
Site-directed mutagenesis		
mClca5_mtp53BS1	AGATAGTTCCCAGATAGATCCACCCCA	CTAAAAATTCCTCTCCAAGGCAACGC
mClca5_mtp53BS2	GAATGTTCTCAAGAGGTGTGACTTAA	AGGACTATGCCTTTTAAAAACATTATT
mClca5_mtp53BS3	TAATATTTAATCAGTGTGCTAAAATCT	GGGATTACGCTCATGATCTCCCCAAGT
Semiquantitative RT-PCR		
CLCA2	CAGATGTGCAGCCTCAGAAG	TGCTGAGCACAGTGGGTAAG
$p21^{WAF1}$	GTTCCTTGTGGAGCCGGAGC	GGTACAAGACAGTGACAGGTC
β2-Microglobulin	CACCCCCACTGAAAAAGATGA	TACCTGTGGAGCAACCTGC